

Modal fields and bending loss analyses of three-layer large flattened mode fibers

Chujun Zhao^{*}, Runwu Peng, Zhixiang Tang, Yunxia Ye, Lei Shen, Dianyuan Fan

*National Laboratory on High Power Laser and Physics, Shanghai Institute of Optics and Fine Mechanics, Chinese Academy of Sciences,
P.O. Box 800-211, Shanghai 201800, China*

Received 17 January 2006; received in revised form 12 April 2006; accepted 21 April 2006

Abstract

Theoretical method to analyze three-layer large flattened mode (LFM) fibers is presented. The modal fields, including the fundamental and higher order modes, and bending loss of the fiber are analyzed. The reason forming the different modal fields is explained and the feasibility to filter out the higher order modes via bending to realize high power, high beam quality fiber laser is given. Comparisons are made with the standard step-index fiber.

© 2006 Elsevier B.V. All rights reserved.

PACS: 42.55.Wd; 42.81.-i

Keywords: High power fiber laser; Large flattened mode fiber; Modal fields; Bending loss

1. Introduction

Output power of high power optical fiber laser is limited by the onset of nonlinear effects, especially stimulated Raman scattering [1]. A common approach for scaling the power and pulse energy is to increase the core size of the fiber and selectively excite only the fundamental mode [2]. But there is an upper limit to the core diameter beyond which single-mode operation is not guaranteed. At NAs lower than 0.06, furthermore, fibers begin to exhibit extremely high bend sensitivity, which imposes a practical lower limit on NA and hence an upper limit on core diameter [3]. Fortunately, many ways have been found to suppress higher-order lasing modes that allow designers to use even larger core diameters wherein essentially multimode fibers can be made to operate with a diffraction-limited beam quality. These techniques include suitably manipulating the fiber index and doping profiles [4,5], using special cavity configurations [6,7], tapering the fiber ends [8], adjusting

the seed launch conditions [9], and coiling the fiber to induce substantial bend loss for all transverse modes other than the fundamental [10].

The magnitude of nonlinearity in an optical fiber depends on the nonlinear refractive index coefficient of the fiber, the power in the optical fiber and the mode confinement. The effective nonlinear coefficient of a fiber can be defined as $n_{\text{nl}}/A_{\text{eff}}$, where n_{nl} is the nonlinear refractive index coefficient and A_{eff} is the effective core area. The nonlinear refractive index coefficient of a fiber depends on the fiber material and as such, it is almost the same for all silica-based fibers. Thus the nonlinearity of the fiber can be reduced by increasing A_{eff} . The large flattened mode (LFM) optical fiber, firstly proposed by Ghatak in 1999, has homogenous modal field in the central region [11]. The schematic of the refractive index profile of the fiber is shown in Fig. 1, where n_1, n_2, n_3 are the refractive indices of the central dip, core and outer cladding and $n_2 > n_1 > n_3$. b, c are the size of the central dip and the core. The design can increase the effective area effectively, which has been discussed and demonstrated in Lawrence Livermore National Laboratory [11,12].

^{*} Corresponding author. Tel.: +86 21 69918809.
E-mail address: c_j_zhao@yahoo.com.cn (C. Zhao).

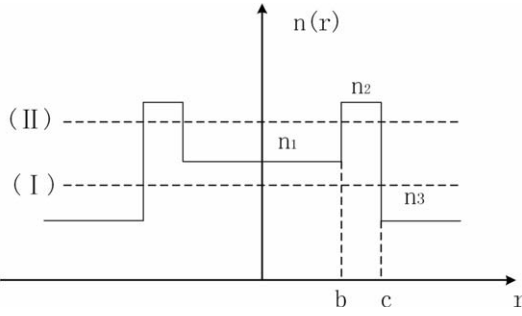


Fig. 1. Schematic of the refractive index profile of the three-layer LFM fiber.

The modal characteristics of the LFM fiber determine its many important properties and bend-induced mode filtering can get high beam quality easily, but there are few papers concerned its modal and bending loss properties, especially higher order modal fields. In the present paper, we will discuss the modal characteristics and bending loss properties of three-layer LFM fibers. The formulations to analyze the LFM fibers are deduced in Section 2. In Section 3, the properties of the modal field and bending loss are studied and comparisons between conventional fiber and LFM fiber are made. Finally, the main results obtained in the paper are summarized.

2. Theoretical analysis

We assume low contrast between the refractive indices, so the dominant modes are mostly linearly polarized; hence all fields are derived from a scalar function ψ , which may stand for the transverse-linearly polarized E field. The longitudinal modal propagation factor $\exp(-i\omega t - i\beta z)$ is neglected in the discussion [13–16].

The refractive index profile analyzed in this paper is shown in Fig. 1, which are named Type I and Type II, respectively. In the analysis, β is the propagation constant of the fiber and $n_{\text{eff}} = \beta/k_0$, where $k_0 = 2\pi/\lambda$, λ is the wavelength. If $n_1 < n_{\text{eff}} < n_2$, we can get

$$\psi = \begin{cases} A_1 I_m(\alpha r) \cos m\phi, & r < b, \\ [A_2 J_m(pr) + A_3 Y_m(pr)] \cos m\phi, & b < r < c, \\ A_4 K_m(\alpha_0 r) \cos m\phi, & r > c, \end{cases} \quad (1)$$

where $\alpha = k_0 \sqrt{n_{\text{eff}}^2 - n_1^2}$, $p = k_0 \sqrt{n_2^2 - n_{\text{eff}}^2}$, $\alpha_0 = k_0 \sqrt{n_{\text{eff}}^2 - n_3^2}$, A_i ($i = 1, 2, 3, 4$) is constant. J_m , Y_m are the Bessel functions of order m , and I_m , K_m are the modified Bessel functions of order m . For the other case, $n_3 < n_{\text{eff}} < n_1$, the corresponding modal fields are

$$\psi = \begin{cases} B_1 J_m(\alpha_1 r) \cos m\phi, & r < b, \\ [B_2 J_m(pr) + B_3 Y_m(pr)] \cos m\phi, & b < r < c, \\ B_4 K_m(\alpha_0 r) \cos m\phi, & r > c, \end{cases} \quad (2)$$

where $\alpha_1 = k_0 \sqrt{n_1^2 - n_{\text{eff}}^2}$, B_i ($i = 1, 2, 3, 4$) are constant.

The boundary conditions at $r = b$ and $r = c$ require merely the continuity of ψ and $\partial\psi/\partial r$, so we can get

$$\frac{\alpha I'_m(\alpha b) J_m(pb) - p I_m(\alpha b) J'_m(pb)}{\alpha I'_m(\alpha b) Y_m(pb) - p I_m(\alpha b) Y'_m(pb)} = -\frac{p J'_m(pc) K_m(\alpha_0 c) - \alpha_0 J_m(pc) K'_m(\alpha_0 c)}{\alpha_0 K'_m(\alpha_0 c) Y_m(pc) - p K_m(\alpha_0 c) Y'_m(pc)}, \quad (3)$$

$$\frac{\alpha_1 J'_m(\alpha_1 b) J_m(pb) - p J_m(\alpha_1 b) J'_m(pb)}{\alpha_1 J'_m(\alpha_1 b) Y_m(pb) - p J_m(\alpha_1 b) Y'_m(pb)} = -\frac{p J'_m(pc) K_m(\alpha_0 c) - \alpha_0 J_m(pc) K'_m(\alpha_0 c)}{\alpha_0 K'_m(\alpha_0 c) Y_m(pc) - p K_m(\alpha_0 c) Y'_m(pc)}. \quad (4)$$

Obviously, for the fundamental modal field absolutely flat in the region $|r| < b$, we must have $d\psi/dr = 0$, $n_{\text{eff}} = n_1$. And thus the modal field distributions are

$$\psi = \begin{cases} C_1, & r < b, \\ C_2 J_0(pr) + C_3 Y_0(pr), & b < r < c, \\ C_4 K_0(\alpha_0 r), & r > c, \end{cases} \quad (5)$$

where C_i ($i = 1, 2, 3, 4$) are constants and n_1, n_2, n_3, b, c must satisfy the following transcendental equation:

$$\frac{J'_0(pb)}{Y'_0(pb)} = -\frac{p J'_0(pc) K_0(\alpha_0 c) - \alpha_0 J_0(pc) K'_0(\alpha_0 c)}{\alpha_0 K'_0(\alpha_0 c) Y_0(pc) - p K_0(\alpha_0 c) Y'_0(pc)}. \quad (6)$$

In calculating the bending loss, we used the method presented by Snyder and co-workers [14,17]. The fiber core and inner claddings are substituted by an equivalent current radiating as an antenna in an infinite medium of index equal to n_N , where n_N is the refractive index of the most external layer for an N -layer fiber. In this article, $N = 3$. To a first approximation and using the Maxwell's equation $\nabla \times \vec{H} = \vec{J} + j\omega\epsilon \vec{E}$, it can be shown that the current density of the equivalent radiating antenna is given by the following expression:

$$\vec{J} = -jk_0 \sqrt{\epsilon_0/\mu_0} [n_N^2 - n^2(r)] \vec{E}(r), \quad (7)$$

where $\vec{E}(r)$ is the exact electric field of the fiber, $n(r)$ the refractive index as a function of the radial coordinate, ϵ_0 the free space dielectric constant, and μ_0 is the free space permeability. As an approximation, it is sufficient to assume that this field is the same as the field of the straight fiber, provided that the bending radius is large enough compared with the fiber dimensions. The fiber is assumed to be bent at a constant radius R_c . The current amplitude I_{co} can be expressed as

$$I_{\text{co}} = -j2\pi k_0 \sqrt{\epsilon_0/\mu_0} \int_0^\infty [n_N^2 - n^2(r')] \psi(r') I_0 \times \left(k_0 \sqrt{n_{\text{eff}}^2 - n_N^2 r'} \right) r' dr', \quad (8)$$

Following the steps of Snyder, the radiated power is expressed as

$$P_{\text{rad}} = \frac{\pi}{2\lambda} n_N \sqrt{\mu_0/\epsilon_0} R_c |I_{\text{co}}|^2 F_{\text{rad}} \times \exp \left\{ -\frac{2k_0 n_N R_c}{3} \left[\left(\frac{n_{\text{eff}}}{n_N} \right)^2 - 1 \right]^{3/2} \right\}, \quad (9)$$

where $F_{\text{rad}} = \frac{1}{(n_{\text{eff}}^2 - n_N^2)^{1/2}} \sqrt{\frac{3\lambda}{8n_N R_c \sqrt{(n_{\text{eff}}/n_N)^2 - 1} [2(n_{\text{eff}}/n_N)^2 + 1]}}$. Thus the loss coefficient is calculated as

$$\gamma = \frac{P_{\text{rad}}}{2\pi R_c P(0)}, \quad (10)$$

where $P(0) = \pi \sqrt{\epsilon_0/\mu_0} \int_0^\infty n(r) |\psi(r)|^2 r dr$ is the power carried by the wave at the fiber input.

3. Results and discussions

The properties of large effective area of the LFM fiber, facilitating lowering the nonlinear effect threshold, have been discussed elsewhere [12]. In this paper, we will mainly discuss its modal field and the bending loss numerically. Considering LFM fibers with different core size $c = 20 \mu\text{m}$, $25 \mu\text{m}$, and $50 \mu\text{m}$, the corresponding central dip sizes are $17.2862 \mu\text{m}$, $22.3418 \mu\text{m}$, and $47.4474 \mu\text{m}$. The

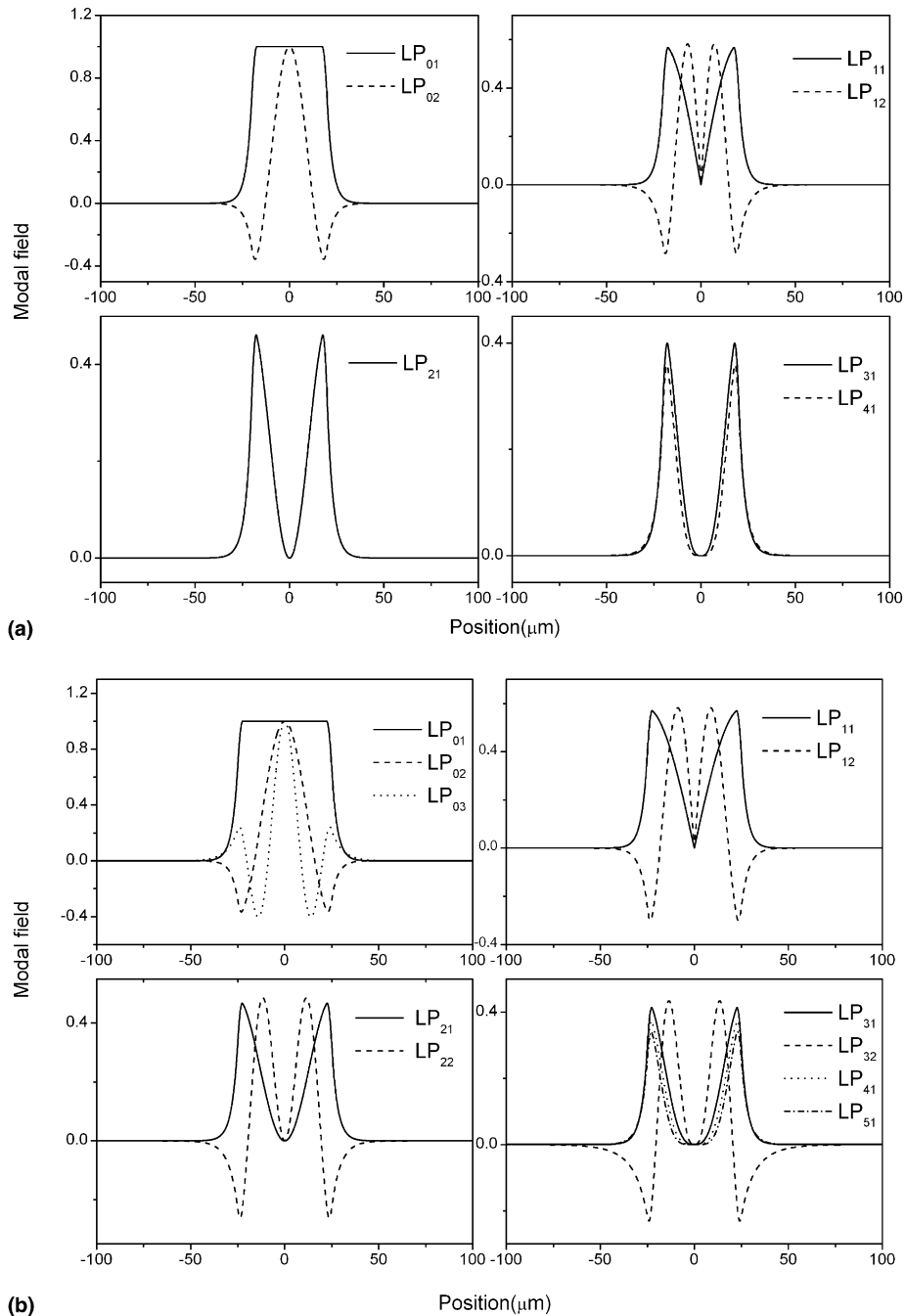


Fig. 2. Modal fields of the LFM fiber with (a) $c = 20 \mu\text{m}$; (b) $c = 25 \mu\text{m}$; and (c) $c = 50 \mu\text{m}$.

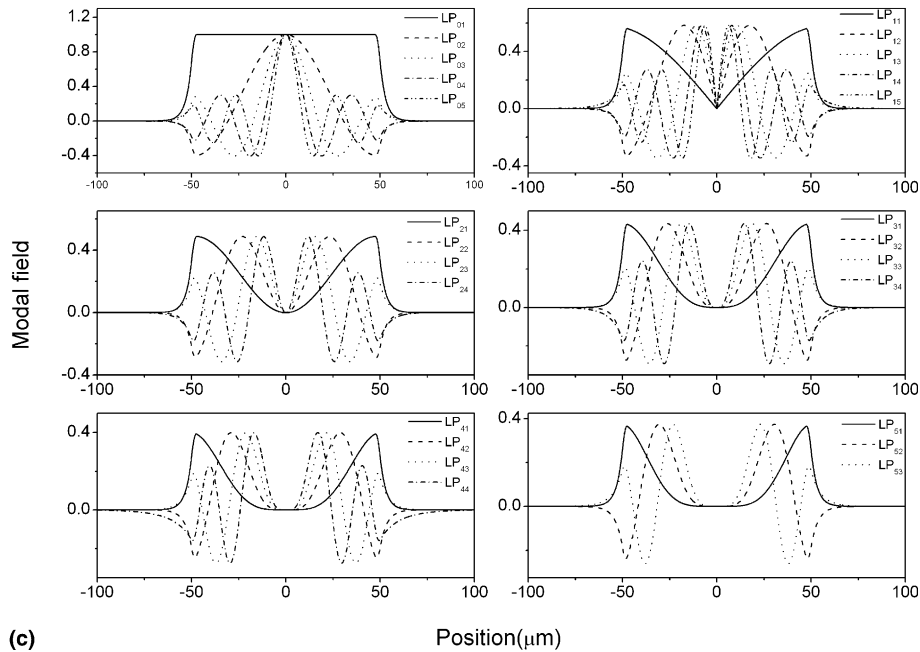


Fig. 2 (continued)

refractive indices can be chosen by using different materials and $n_1 = 1.458$, $n_2 = 1.459$, and $n_3 = 1.457$ in this calculation [12]. The other parameters are $\lambda = 1.06 \mu\text{m}$, $A_1 = B_1 = C_1 = 1$.

3.1. Modal fields

Fig. 2 shows the fundamental and higher order modal fields with $c = 20 \mu\text{m}$, $25 \mu\text{m}$, and $50 \mu\text{m}$. It can be seen clearly that increasing c makes the LFM fiber accommodate more modes. For the LFM fibers, light trace in the core is quite different from that in a standard step-index fiber. At the interface of central dip and the core, reflection and refraction occur because the index of central dip is lower than that of the core. Part of the light energy leaks away from the central dip because total internal reflection (TIR) is not satisfied. Energy redistribution takes place as light propagates along the fiber. Finally, a stable homogeneous intensity distribution of the fundamental mode is formed. For other modes with $m = 0$, the modal field begins to oscillate and the intensity is not zero at the center. With increasing modal order $m (> 0)$, the fields shift towards the fiber border having no intensity in the center of the fiber. The larger the m is, further away the modal field shifts.

The LFM refractive index profile differs from the step-index profile by the inclusion of a ring raised in refractive index above the inner core. To clarify the modal field characteristics of LFM fiber, the discussed LFM fiber with $c = 25 \mu\text{m}$ and the step-index fiber with the same core size and a flat refractive index of 1.458 across the entire core are considered and comparisons are made, as shown in Fig. 3. We plot the modal profiles of modes LP_{01} , LP_{11} ,

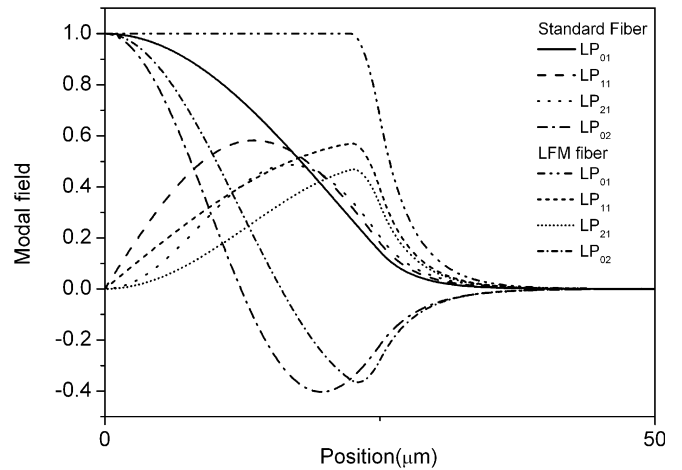


Fig. 3. Modal field comparisons between standard step-index and LFM fiber.

LP_{21} , and LP_{02} of the LFM and the standard step-index fiber, respectively. It can be seen that the modal fields of the LFM fiber have a much more obvious tendency shifting towards fiber border than the step-index fiber. The phenomenon correlates with the raised refractive index ring of the LFM fiber.

3.2. Bending loss

The LFM fiber is an ideal candidate for the high power fiber laser for its large effective area. With power scaling, maintaining high beam quality is imperative, while bending the fiber provides the easiest method to filter out the higher order modes.

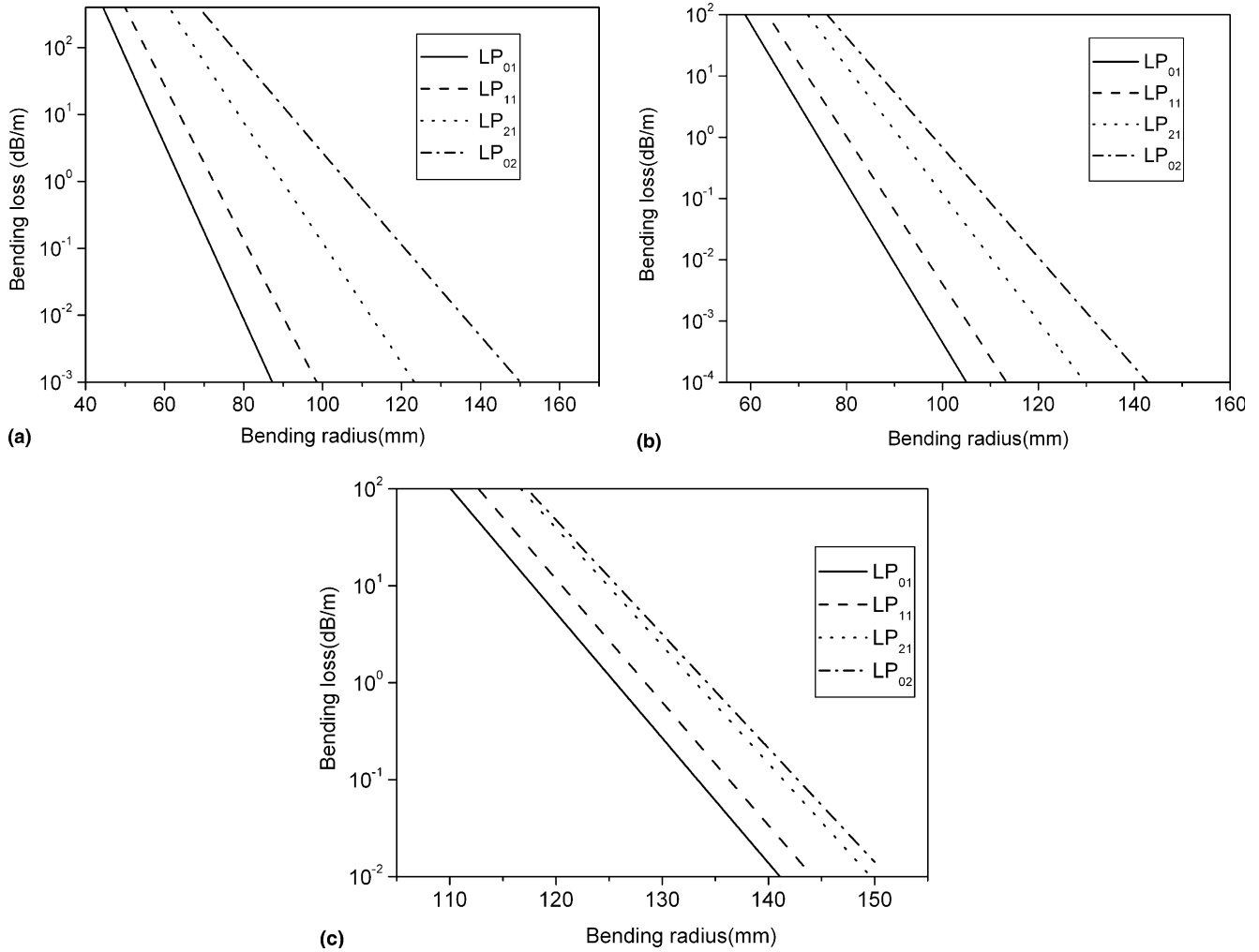


Fig. 4. Bending radius vs. bending loss for the LFM fibers with (a) $c = 20 \mu\text{m}$; (b) $c = 25 \mu\text{m}$; and (c) $c = 50 \mu\text{m}$.

The four lowest order modes of the fiber are LP_{01} , LP_{11} , LP_{21} , and LP_{02} . Fig. 4 shows the relationship of the bending loss of these four modes versus different bending radius. Among these modes, LP_{02} mode has the largest bending loss and LP_{01} mode suffers the smallest loss. Moreover, it can be found that the bending loss decreases with increasing bending radius. These results can be explained by Eqs. (9) and (10) in Section 2. From Eq. (9) it is clear that the closer is n_{eff} to n_3 , the higher will be the bending loss for a fixed bending radius. For these modes, LP_{02} mode has the smallest n_{eff} , which is the nearest one to n_3 , so it has the largest bending loss. LP_{01} mode has the largest n_{eff} . Combining Eqs. (9) and (10), it can be found that the bending loss decreases exponentially with increasing bending radius. With core size increasing, it is well known that the fiber can accommodate more modes and the difference between modes becomes small [17], so the bending loss difference between modes gets small, as also can be understood from Eq. (9) and has been shown in Fig. 4.

Bending loss comparisons are made between the LFM and standard step-index fiber. The parameters used are

the same with Fig. 4. It can be seen from Fig. 5 that the LP_{01} modes of the two fibers suffer nearly the same bending loss, but for the higher order modes, the standard

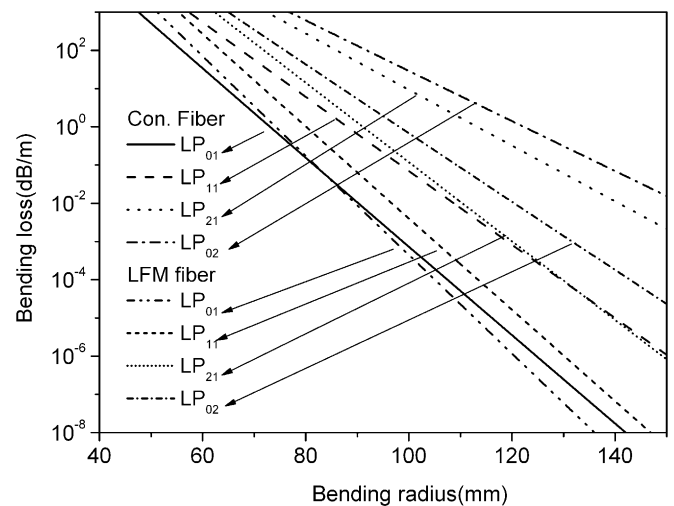


Fig. 5. Bending loss comparisons between standard step-index and LFM fiber.

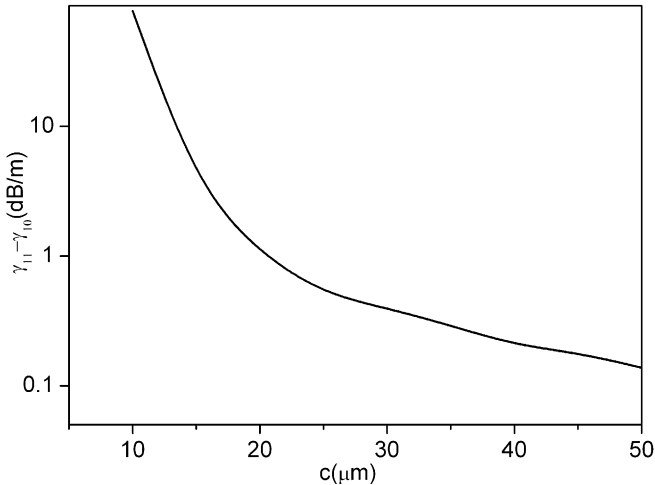


Fig. 6. Calculated values of the LP₁₁ suppression relative to LP₀₁ versus c at the indicated values of $\gamma_{01} = 1$ dB/m.

step-index fiber has larger bending loss than the LFM one. These results result from the raised refractive index ring of the LFM fiber, which makes the LFM fiber has larger n_{eff} than the standard step-index fiber for the same mode. Furthermore, different n_{eff} determines the different bending loss. The difference between n_{eff} of LP₀₁ modes is small and therefore the two kinds of fibers have nearly the same bending loss. For higher order modes, the LFM fiber has much larger n_{eff} than the standard step-index one for the same mode, so it has smaller bending loss. Therefore, bend-induced mode filtering is more efficient for the step-index fiber, but the LFM fiber outweighs the step-index one by its much larger effective area.

Following the analysis in Ref. [10], we calculated the bending loss for LP₁₁ (γ_{11}) as a function of fiber core radius for specified values of LP₀₁ bending loss (γ_{01}) 1 dB/m, as shown in Fig. 6. With the increasing core size, the LP₁₁ suppression relative to LP₀₁ becomes small for fiber with large core size can hold more modes. If the core size is small, bending the fiber can filter out the higher order modes efficiently. If large, simply bending the fiber can hardly get ideal filtering effect and we must adopt other measures. If we assume that the loss difference of 1 dB/m can discriminate LP₁₁ from LP₀₁, the ideal core size is better less than 40 μm . The calculation provides a conservative estimate of γ_{11} relative to γ_{01} . For the influences of the rare earth doping, we have not discussed here.

4. Conclusions

In the article, the properties of the LFM fiber, including the fundamental and higher order modal fields, and bending loss are discussed by the theoretical method presented. The reasons forming the different modal field is explained by whether the TIR is satisfied. The feasibility to filter out the higher order modes via bending is given. Compared with the standard step-index fiber, the LFM one shows more obvious shifting behavior towards fiber border for its modal field and smaller bending loss for the higher order modes. It also can be seen that bending the LFM fiber is an efficient way to get good beam quality for the LFM fiber with core size less than 40 μm in high power fiber laser applications. For larger core size, we must adopt other measures to get ideal beam quality.

Acknowledgement

This work was partially supported by the Natural Science Foundation of China (Grant Nos. 10576012 and 60538010).

References

- [1] G.P. Agrawal, *Nonlinear Fiber Optics*, Academic, Boston, 1989.
- [2] M.E. Fermann, *Opt. Lett.* 23 (1998) 52.
- [3] A. Carter, B. Samson, *Mil. Aerosp. Electron.* 2 (2005).
- [4] H.L. Offerhaus, N.G. Broderick, D.J. Richardson, R. Sammut, J. Caplen, L. Dong, *Opt. Lett.* 23 (1998) 1683.
- [5] T. Bhutta, J.I. Mackenzie, D.P. Shepherd, R.J. Beach, *J. Opt. Soc. Am. B* 19 (2002) 1539.
- [6] U. Griebner, R. Koch, H. Schonngel, R. Grunwald, *Opt. Lett.* 21 (1996) 266.
- [7] U. Griebner, H. Schonngel, *Opt. Lett.* 24 (1999) 750.
- [8] J.A. Alvarez-Chavez, A.B. Grudinin, J. Nilsson, P.W. Turner, W.A. Clarkson, *CLEO (1999)* 247.
- [9] I. Zawischa, K. Plamann, C. Fallnich, H. Welling, H. Zellmer, A. Tunnermann, *Opt. Lett.* 24 (1999) 469.
- [10] J.P. Koplow, D.A.V. Kliner, L. Goldberg, *Opt. Lett.* 25 (2000) 442.
- [11] A.K. Ghatak, I.C. Goyal, R. Jindal, *SPIE Proc.* 3666 (1999) 40.
- [12] J.W. Dawson, R. Beach, I. Jovanovic, B. Wattellier, Z. Liao, S.A. Payne, C.P.J. Barty, *SPIE Proc.* 5335 (2004) 132.
- [13] R.K. Varshney, A.K. Ghatak, I.C. Goyal, S.C. Antony, *Opt. Fiber Tech.* 9 (2003) 189.
- [14] H.T. Hattori, A. Safaai-Jazi, *Appl. Opt.* 37 (1998) 3190.
- [15] A. Safaai-Jazi, H.T. Hattori, J.A. Baghdadi, *SPIE Proc.* 3666 (1999) 30.
- [16] S.F. Mahmoud, A.M. Kharbat, *J. Light. Tech.* 11 (1993) 1717.
- [17] A.W. Snyder, J.D. Love, *Optical Waveguide Theory*, Chapman & Hall, London, 1983.